Study on denoising of continuous spectrum on-line monitoring signal of water quality with micro-reagents based on HHT[*]

LI Wen, LÜ Binbin**, FU Hao, and CAI Yongqing
Institute of Mechanical and Electrical Engineering, North China University of Technology, Beijing 100144, China

A continuous spectrum water quality on-line monitoring signal processing method based on Hilbert-Huang transform (HHT) is proposed in this paper, which combines the micro-reagent water quality on-line monitoring technology of sequential injection. The modulation signal and spectrum curve of each intrinsic mode function (IMF) component of the original spectrum signal were obtained by empirical mode decomposition (EMD). The water sample data of different concentrations in the continuous spectrum on-line monitoring system was analyzed by the HHT model. The noise signal was excavated to realize the noise reduction processing, and the reconstruction of the continuous spectrum signal was realized after the noise reduction processing was completed. The research results show that this method can effectively reduce the noise of continuous spectrum signals according to different signal-to-noise characteristics of continuous spectrum, and has convenient use, fast processing speed, and high resolution in the time-frequency domain, which effectively improves the stability and accuracy of the micro-reagent continuous spectrum water quality on-line monitoring system.

The spectral analysis method[1-3] has been applied in certain on-line monitoring fields. The spectrometer is affected by external environment such as temperature, humidity, and electrical noise, and there is interference such as stray light inside. Therefore, many irrelevant noise signals are obtained from the data collected by the spectrometer in addition to the useful signals, and the applications of continuous spectrum on-line detection are subject to certain restrictions. If the noise of the spectral analysis data is not eliminated, it will affect or even mask the real signal, thereby affecting the quality of the calibration model and the accuracy of predicting unknown samples[4-6]. HUANG et al[7] have proposed a new method for adaptively processing non-linear and non-stationary signals Hilbert-Huang transform (HHT). This method only needs to decompose the signal by empirical mode decomposition (EMD) according to the characteristics of the signal itself to obtain multiple intrinsic mode function (IMF) components. The Hilbert transform is performed on these components to complete the local feature description of the signal in the time-frequency domain. Therefore, it is very suitable for the noise reduction analysis of non-linear and non-stationary spectral signals[8-11]. PENG et al[12,13] have analyzed the denoising effect of HHT on the signal of vortex flowmeter and double-triangle bluff body vortex flowmeter in oscillating flow under different signal-to-noise ratio conditions. WANG et al[14] have found that using Hilbert spectrum analysis of denoising data can clearly identify the natural frequency of the bridge structure, which was consistent with theoretical calculations, and the proposed method can effectively determine the natural vibration characteristics of the bridge structure. YANG et al[15] have used HHT to process the fluorescent optical fiber temperature measurement signal, and a good noise reduction effect has been achieved.

The water quality total nitrogen and total phosphor parameters were studied as an example in this paper, the signal noise reduction processing method was based on the HHT, and the noise reduction analysis of the water quality spectrum signal was studied.

The EMD is to perform multiple adaptive decompositions to separate out the IMF according to the characteristics of the signal itself[16]. The IMF must satisfy that the difference between the number of extreme points of the original signal and the number of intersection points of the original signal with the horizontal axis cannot be greater than 1, and at any point, the mean value equal to 0 is determined by the envelope defined by the maximum value and the minimum value.

The formula in mathematics indicates that the decomposition process is the sum of n intrinsic modal function $c_j(x)$ components and a residual $R_n(x)$, namely

$$f(x) = \sum_{j=1}^{n} c_j(x) + R_n(x). \qquad (1)$$

Hilbert transform is an important means for HHT to perform spectrum analysis. All IMF components were obtained by decomposing the analyzed signal after improvement, and it needs to perform the Hilbert transform. The signal will present 90° phase shift after Hilbert transform. The continuous spectrum vector is represented by $f(x)$, which is transformed into $H[f(x)]$ after Hilbert transformation[17] as

$$H[f(x)] = \frac{1}{\pi} \int_{-\infty}^{+\infty} \frac{f(t)}{x-t} dt, \qquad (2)$$

where $H[f(x)]$ is the convolution of $f(x)$ and $\frac{1}{\pi x}$, x is Band number, and t is integral variable.

When the signal is analyzed, the Hilbert transform is not used to avoid the influence of the remaining items on other IMF components. The corresponding Hilbert spectrum is obtained by Hilbert change of the signal expression composed of each IMF as

$$H(w,x) = \text{Re} \sum_{i=1}^{n} a_i(x) e^{j\int w_j(x)dx}, \qquad (3)$$

where $a(x)$ is the instantaneous amplitude.

The signal expression is analyzed and processed by the HHT algorithm. Combine time and frequency for analysis in time domain or frequency domain, which is not possible with the Fourier transform. At the same time, each IMF component obtained by signal decomposition of EMD contains different time feature scales and frequencies, good local time-frequency characteristics, and high resolution.

As shown in Fig.1, the continuous spectrum on-line detection technology of water quality was applied to this experiment, which includes sequential injection module, data processing display and system control module, high temperature closed digestion module, and light source detection module. The sequential injection module includes a syringe pump and a multi-channel switching valve island. Its minimum liquid inlet accuracy is 0.002 5 mm/1.038 1 μL, the syringe specification is 500 μL, and the valve head model is M07. The compact deuterium-halogen tungsten light source is used in the light source detection module. The emission spectrum range of the light source is 190—2 500 nm. The AVANTES high-resolution spectrometer has a response range of 180—1 200 nm. The design of the digestion tank in the high temperature closed digestion module should aim at low power consumption, low cost, and miniaturization. The digestion tank should have the characteristics of small size, convenient processing, fast heating to the required digestion temperature, fast heat dissipation, and at the same time the digestion tank is also used as a detection tank[18].
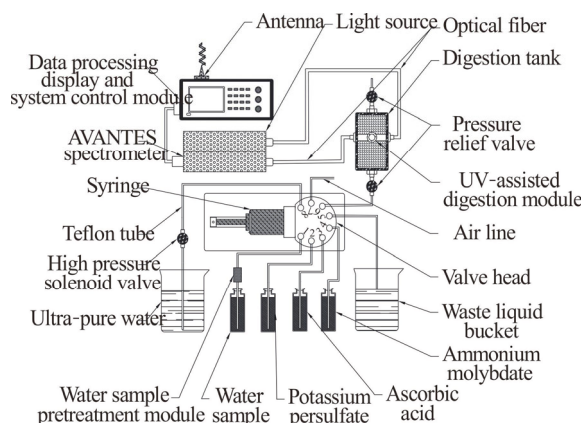

Fig.1 Schematic diagram of continuous spectrum on-line monitoring

The experiment needs to be prepared for 1 μL—1 mL research plus a single-channel pipette. The XP205 electrode is prepared with an electronic balance with an accuracy of 0.1 and a desiccator.

The concentration gradient of total nitrogen solution is set to 0.4 mg·L^{-1}, and its concentration range is 0—2 mg·L^{-1}, that is, there are 6 gradients of 0.0 mg·L^{-1}, 0.4 mg·L^{-1}, 0.8 mg·L^{-1}, 1.2 mg·L^{-1}, 1.6 mg·L^{-1}, and 2.0 mg·L^{-1}. There are 6 groups of experimental subjects in the same gradient, a total of 36 groups of experimental subjects. The concentration gradient of total phosphorus solution is set to 0.2 mg·L^{-1}, and its concentration range is 0—1 mg·L^{-1}, that is, there are 6 gradients of 0.0 mg·L^{-1}, 0.2 mg·L^{-1}, 0.4 mg·L^{-1}, 0.6 mg·L^{-1}, 0.8 mg·L^{-1}, and 1.0 mg·L^{-1}. There are 6 groups of experimental subjects in the same gradient, a total of 36 groups of experimental subjects.

The collection of spectral signals within a certain range is due to the detection unit composed of a compact deuterium-halogen tungsten light source and a high-resolution spectrometer, and the overall size of the detection device is taken into account, so the digestion cell is regarded as the measurement cell. The absorbance A of each standard water sample (finally analyzing the corresponding parameter in the water sample from the curve of each parameter) can be obtained according to Lambert-Beer law, namely

$$A = \lg(\frac{1}{T}) = KBC = -\lg(\frac{sample - Dark}{reference - Dark}) \times 100\%, \quad (4)$$

where A is the absorbance of water sample, T is the media transmittance, K is the molar absorption coefficient, B is the optical path, C is the concentration, $reference$ is the photoelectric signal when the light source is on, $Dark$ is the photoelectric signal when the light source is off, and $sample$ is the photoelectric signal after reagent digestion.

The above-mentioned working point solution is taken to the digestion tank according to the concentration from low to high, and the parameters are detected by using sequential injection technology. The total nitrogen reagent

performs spectral scanning after the system is digested and dropped to normal temperature. The ultraviolet absorption peak of nitrate nitrogen is about 202.0 nm in the full spectrum wavelength range, and the wavelength of total phosphor is about 730.0 nm, as shown in Fig.2.
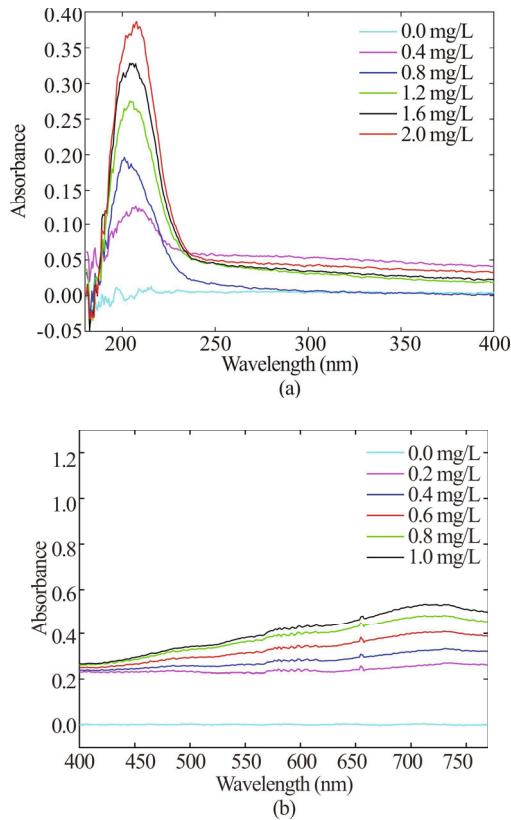

Fig.2 Absorption spectra of raw signals for (a) total nitrogen and (b) total phosphor

The noise generated by the spectrometer belongs to the "non-linear and non-stationary" signal. The EMD of the spectral signal is based on the requirements of the Hilbert transform. The Hilbert transform and spectrum analysis are performed after the IMF components are obtained. The data signal with a concentration of 0.8 mg·L^{-1} in the total nitrogen spectrum is randomly selected, as shown in Fig.3. The 6 IMFs and one remaining term are obtained by EMD, as shown in Fig.4.
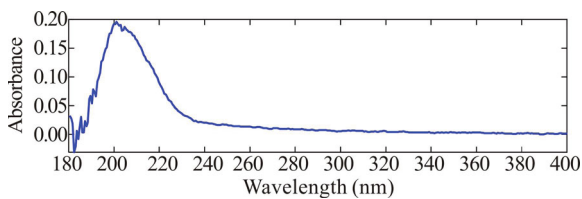

Fig.3 Spectral signal of total nitrogen with concentration of 0.8 mg·L⁻¹ to be decomposed

As shown in Fig.4, the spectral signal is decomposed into 6 different frequencies from high to low, different scale intrinsic mode functions IMF1—IMF6, and a re-

maining term, of which the signal fluctuations in IMF1 and IMF2 are mainly concentrated in 180—250 nm range. The value of the remaining term obtained by EMD does not change significantly, and the result is a monotonic function, which proves that it is completely decomposed.
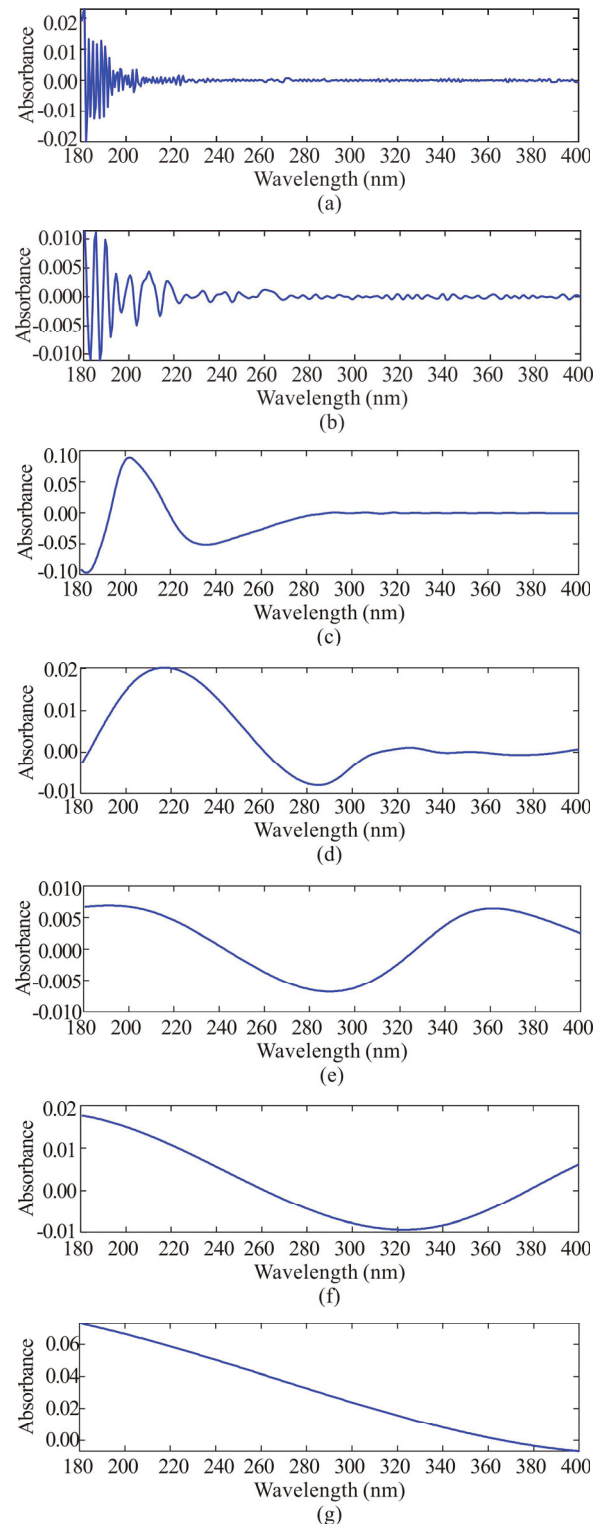

Fig.4 EMD for (a) IMF1 signal, (b) IMF2 signal, (c) IMF3 signal, (d) IMF4 signal, (e) IMF5 signal, (f) IMF6 signal, and (g) remaining term signal

As shown in Fig.5, the Hilbert transform of each IMF component decomposed by EMD is based on the HHT principle and algorithm. The new analytical signal spectrum is constructed by the Hilbert transform result of the spectral signal, and the corresponding instantaneous frequency of each IMF component is obtained. A large number of irregular peak frequencies are contained by the instantaneous frequency of the IMF1 component, which changes rapidly with wavelength. Similarly, IMF2 also concentrated on some irregular peaks in the middle and end parts, which tended to be more stable than the IMF1 frequency changes. The instantaneous frequencies of IMF3 and IMF4 components fluctuate mainly at the wavelength of 320—350 nm, and the other wavelengths are basically in a stable state. The instantaneous frequencies of IMF5 and IMF6 components are in a stable state except for the two ends.
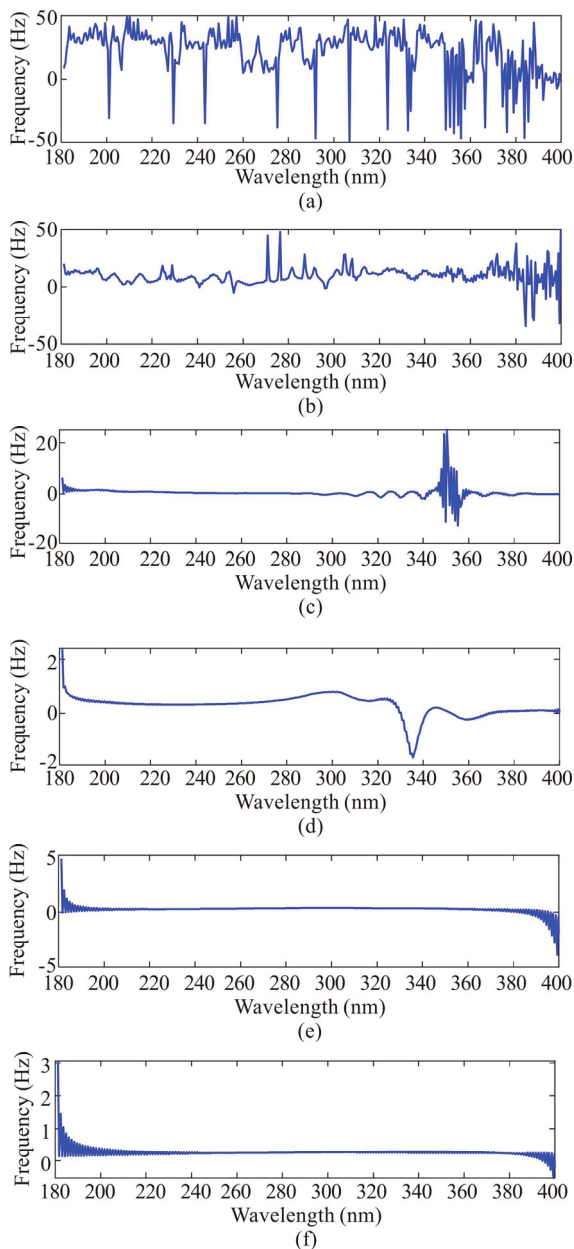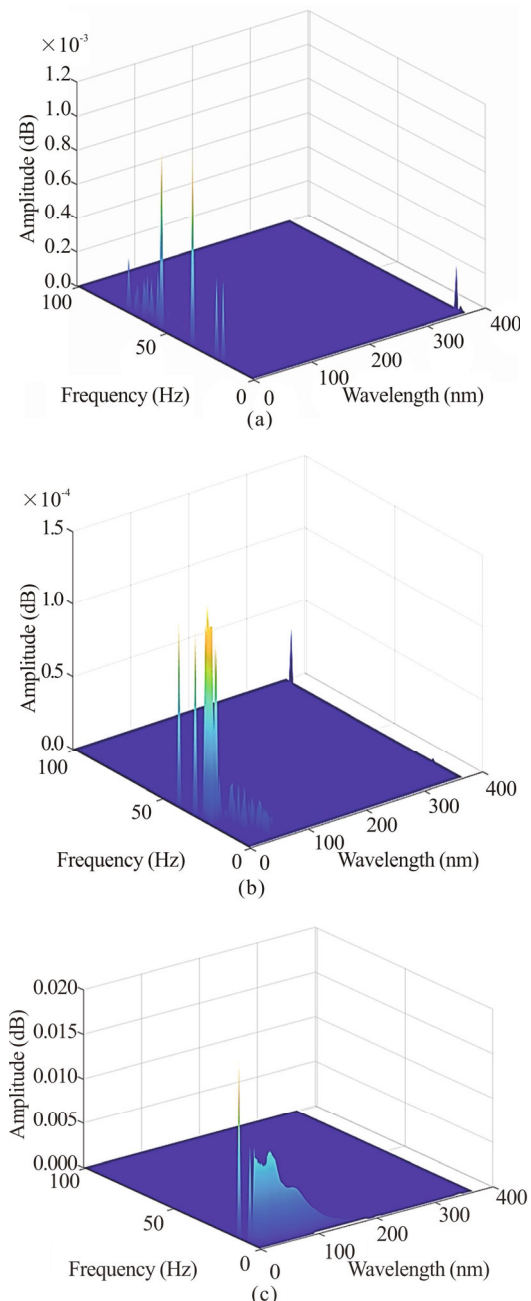
Fig.5 Instantaneous frequencies of (a) IMF1 signal, (b) IMF2 signal, (c) IMF3 signal, (d) IMF4 signal, (e) IMF5 signal, and (f) IMF6 signal

As shown in Fig.6, the corresponding Hilbert spectrum analysis was performed on each IMF component. The distribution trend of each IMF spectrum decomposed by the spectrum signal is generally from high to low, and the spectrum changes are mainly concentrated in the front part of the wavelength range. There are obvious differences in the frequency spectrum of IMF1 to IMF6, and there is a part of overlap. The absorbance information at the wavelength of about 202 nm is extracted in this experiment, which plays a vital role in filtering the noise at the front end of the wavelength range and the accuracy of the experimental results[19,20].
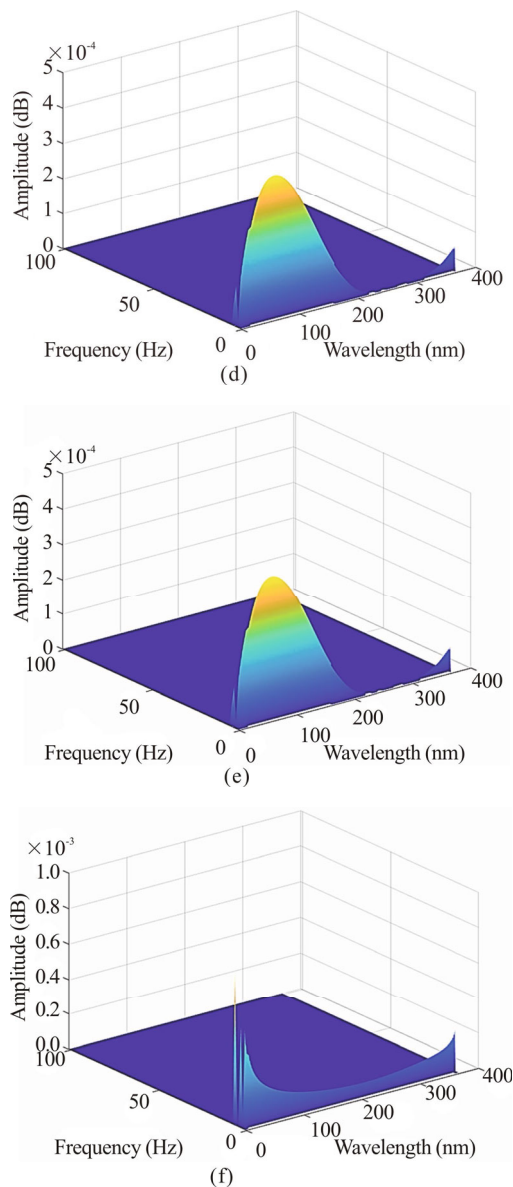
(d)

(e)

(f)

Fig.6 Hilbert spectra of (a) IMF1 signal, (b) IMF2 signal, (c) IMF3 signal, (d) IMF4 signal, (e) IMF5 signal, and (f) IMF6 signal

The instantaneous frequency and Hilbert spectrum of each IMF were decomposed by analyzing the spectral signal. The frequency of the noise component in the signal is much higher than the signal frequency, and it is mainly distributed in IMF1 and IMF2. Therefore, the noisy inherent modal functions IMF1 and IMF2 were filtered, and other noise-free components were retained, and the filtered IMF components are linearly superimposed, and the result of the total nitrogen spectrum signal with a concentration of 0.8 after filtering the noise is obtained, as shown in Fig.7.

The noise reduction of the continuous spectrum signal was processed using the above method, and the HHT analysis was performed on other concentration parameters in the total nitrogen and total phosphorus. The filtered results of the original spectral signals of different

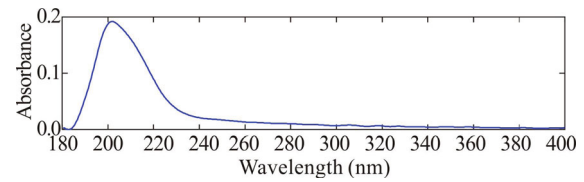concentrations were obtained and reconstructed, as shown in Fig.8.

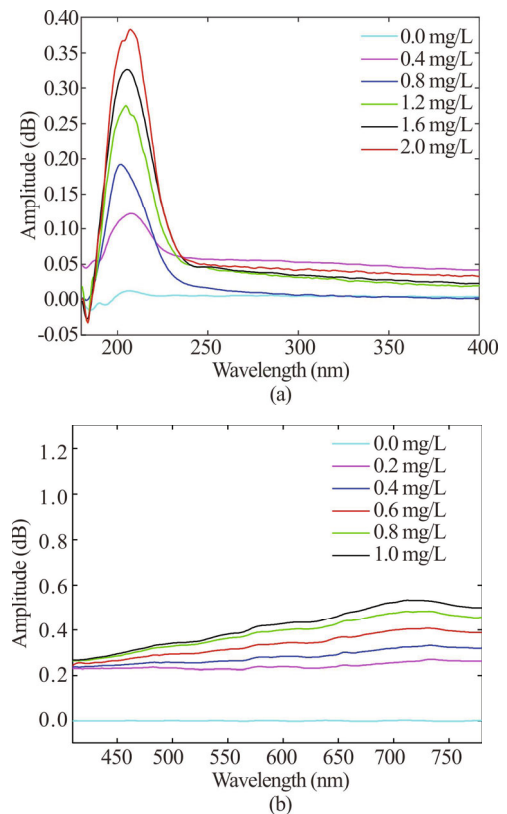**Fig.7 The spectral signal after noise reduction**

(a)

(b)

Fig.8 Reconstruction of spectral signals for (a) total nitrogen and (b) total phosphor

The original spectral signal and the spectral signal after HHT noise reduction processing are curve-fitted to the obtained data with absorbance as the ordinate and concentration as the abscissa, and the curve is obtained as shown in Fig.9.

The concentration and gradient have 6 groups of parallel experiments according to the experimental content. Therefore, the standard deviations of the standard operating points of each parameter are counted and reflected in the form of error bars on each standard operating point in Fig.9. As shown in Fig.9(b) and (d), the measured data is subjected to HHT noise reduction processing and then drawn as a curve for comparison. The total nitrogen and total phosphorus indices are more accurate after HHT noise reduction treatment, and the deviation from the fitted curve is not much different, so the drawn standard working curve is reliable and accurate after HHT noise reduction treatment.
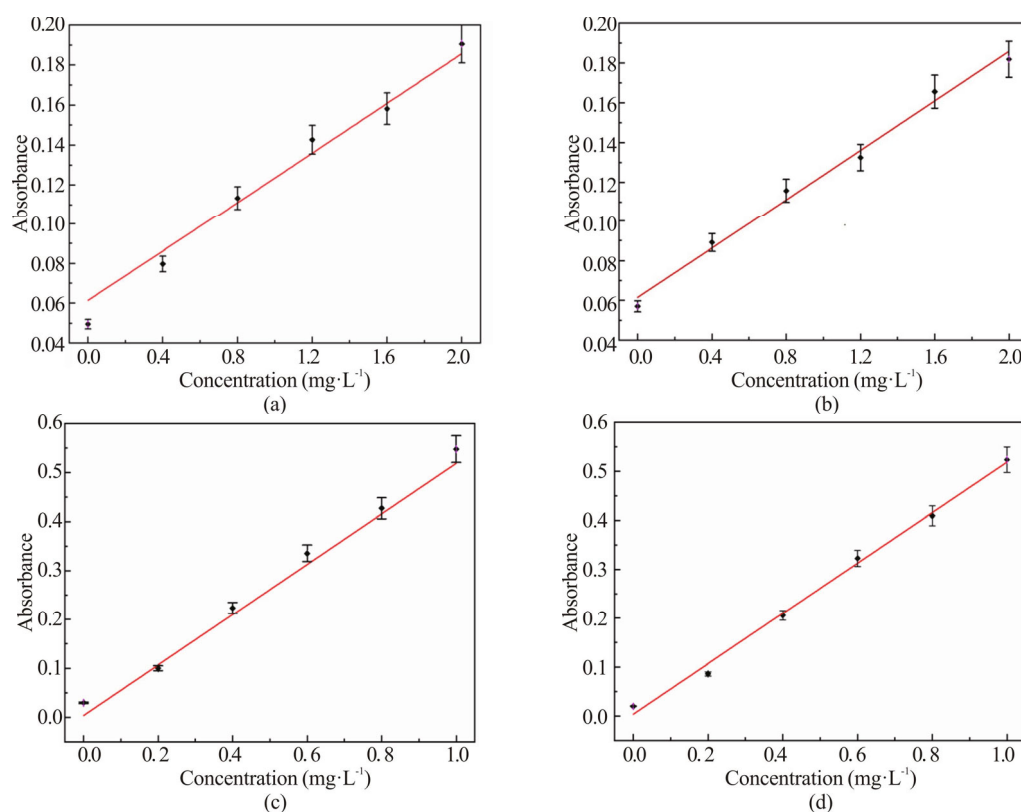
Fig.9 Original spectral data for (a) total nitrogen and (c) total phosphor; HHT processed results for (b) total nitrogen and (d) total phosphor

Tab.1 Work curve related parameters

Parameter	Fitting function	Adjusted R-square	Residual sum of squares
TN (Raw data)	$y=0.061\ 3x+0.060\ 1$	0.979 6	0.000 096 9
TN (Data processed by HHT)	$y=0.062\ 2x+0.061\ 4$	0.990 9	0.000 092 8
TP (Raw data)	$y=0.520\ 3x+0.008\ 5$	0.980 6	0.000 085 3
TP (Data processed by HHT)	$y=0.514\ 8x+0.003\ 6$	0.995 4	0.000 086 1

The 10 mg·L⁻¹ potassium nitrate standard solution was prepared according to the national standard and the deionized water of grade EW-I in the "GB 11446-1-2013 National Standard for Deionized Water". The total nitrogen standard water sample solution is configured to contain 0.2 mg·L⁻¹, 0.6 mg·L⁻¹ and 1.0 mg·L⁻¹, and each standard solution gradient contains 6 sets of parallel experiments. The total phosphorus standard water sample solution is configured to contain 0.1 mg·L⁻¹, 0.3 mg·L⁻¹ and 0.5 mg·L⁻¹, and each standard solution gradient contains 6 sets of parallel experiments. The continuous spec-

trum on-line monitoring technology is used for the concentration from low to high, and the parameters are detected. HHT noise reduction is performed on each set of data, and then the relative standard deviation (RSD) of each parameter is calculated. At the same time, the national standard method is used to detect each parameter separately, and the RSD is obtained, then the repeatability of HHT noise reduction processing method with the original spectral data and the national standard method is analyzed and compared. The RSD of each parameter is shown in Tab.2.

Tab.2 RSD comparison of total nitrogen and total phosphor experiments

TN (mg·L⁻¹)	Data processed by HHT RSD (%)	Raw data RSD (%)	GB (code) RSD (%)	TP (mg·L⁻¹)	Data processed by HHT RSD (%)	Raw data RSD (%)	GB (code) RSD (%)
0.20	3.43	3.69	3.23	0.10	1.93	2.05	1.87
0.60	3.35	3.48	3.19	0.30	2.01	2.14	1.92
1.00	3.42	3.82	3.21	0.50	2.17	2.23	2.05

The repeatability of total nitrogen and total phosphorus parameters is similar to that of the national standard method. And after HHT noise reduction processing, the repeatability is significantly improved. The reliability and stability of HHT noise reduction processing have been proven, as shown in Tab.2.

The HHT is adaptive in the noise reduction processing of continuous spectrum signals. It can perform unique EMD according to the characteristics of the signal itself, and the local characteristics in the time domain and frequency domain are maintained at the same time. The water quality total nitrogen and total phosphorus parameters are studied as an example in this paper, and the signal noise reduction processing method is based on the HHT and fusion continuous spectrum water quality online monitoring technology. The Hilbert transform is carried out after EMD, the continuous spectrum signal is analyzed by Hilbert spectrum, and finally the different concentration spectrum signals after the noise reduction process are reconstructed. The comparative analysis of the experimental results found that the correlation coefficient of the total nitrogen parameter fitting curve increased from 0.979 6 to 0.990 9, an increase of 1.15%. The total phosphorus parameter fitting curve increased from 0.980 6 to 0.995 4, an increase of 1.5%. Three different concentrations of total nitrogen and total phosphorus *RSD* increased significantly. Therefore, the method can effectively remove the noise in the signal, and has the characteristics of convenient use, fast processing speed, and high time-frequency domain resolution, which improves the stability and accuracy of continuous spectrum online monitoring technology.

Statements and Declarations

The authors declare that there are no conflicts of interest related to this article.

References

[1] HARVIE A J, DEMELLO J C, et al. Optical determination of flow-rate and flow-uniformity in segmented flows[J]. Chemical engineering journal, 2020, 394：124908.

[2] YIN M Q, HU X F, SUN Y N, et al. Broad-spectrum detection of zeranol and its analogues by a colloidal gold-based lateral flow immunochromatographic assay in milk[J]. Food chemistry, 2020, 321：126697.

[3] HAN B, ZHANG Y N, WANG X, et al. Non-contact flow rate detection of component in mixed gas using spectrum absorption theory[J]. Optical fiber technology, 2018, 45：167-172.

[4] ZHANG R R, MA S, ERDAL S, et al. Hilbert-Huang transform analysis of dynamic and earthquake motion recordings[J]. Journal of engineering mechanics, 2003, 129(8)：861-875.

[5] WU Z H, HUANG N E. A study of the characteristics of white noise using the empirical mode decomposition method[J]. The royal society, 2004, 460：1597-1611.

[6] ZHAO Y, ZHANG H W. Displacement measurement method based on laser self-mixing interference in the presence of speckle[J]. Chinese optics letters, 2020, 18(5)：051201.

[7] HUANG N E, ZHENG S, LONG S R. A new view of non-linear water waves—Hilbert spectrum[J]. Annual review of fluid mechanics, 1999, 31：417-457.

[8] HUANG N E, ZHENG S, LONG S R, et al. The empirical mode decomposition and Hilbert spectrum for non-linear and nonstationary time series analysis[J]. The royal society, 1998, 454：903-995.

[9] CHEN H K, WANG T F, WU S S, et al. Research on separation and enhancement of speech micro-vibration from macro motion[J]. Optoelectronics letters, 2020, 16(06)：462-466.

[10] LUPIERI G, CONTENTO G. Numerical simulations of 2-D steady and unsteady breaking waves[J]. Ocean engineering, 2015, 106：298-316.

[11] FAN G, ZHANG J J, FU X, et al. Dynamic failure mode and energy-based identification method for a counter-bedding rock slope with weak intercalated layers[J]. Journal of mountain science, 2016, 13(12)：2111-2123.

[12] PENG J. Hilbert-Huang transform (HHT) based analysis of signal characteristics of vortex flowmeter in oscillatory flow[J]. Flow measurement & instrumentation, 2012, 26(4)：37-45.

[13] PENG J, FANG M. Response of a dual triangulate bluff body vortex flowmeter to oscillatory flow[J]. Flow measurement and instrumentation, 2014, 35：16-27.

[14] WANG X P, HUANG S X, KANG C, et al. Integration of wavelet denoising and HHT applied to the analysis of bridge dynamic characteristics[J]. Applied sciences, 2020, 10(10)：3605.

[15] YANG Y J, WANG Z Y, YANG X P, et al. Signal processing of fluorescent optical fiber temperature measurement based on Hilbert-Huang transform[J]. Advanced materials research, 2014, 1052：447-453.

[16] ZHANG X J, HUO Y, WAN D S. Improved EMD based on piecewise cubic Hermite interpolation and mirror extension[J]. Chinese journal of electronics, 2020, 29(05)：899-905.

[17] YANG K M, WANG G P, FU P J, et al. A model on extracting the pollution information of heavy metal copper ion based on the soil spectra analyzed by HHT in time-frequency[J]. Spectroscopy and spectral analysis, 2018, 38(2)：564. (in Chinese)

[18] LI W, WANG L M, CHANG L, et al. Sequential injection-continuous spectroscopy based multi-parameter method for water quality analysis[J]. Spectroscopy and spectral analysis, 2021, 41(02)：612-617.

[19] DONG Z K, SONG Y R, XU R Q, et al. Broadband spectrum generation with compact Yb-doped fiber laser by intra-cavity cascaded Raman scattering[J]. Chinese optics letters, 2017, 15(07)：80-83.

[20] ZHU X B. A novel FBG velocimeter with wind speed and temperature synchronous measurement[J]. Optoelectronics letters, 2018, 14(04)：276-279.